

Novel ATP-competitive MEK inhibitor E6201 is  
effective against vemurafenib-resistant melanoma  
harboring the MEK1-C121S mutation  
in a preclinical model.

(MEK1-C121S 変異を持つ  
vemurafenib 耐性メラノーマにおける  
ATP 競合型 MEK 阻害剤 E6201 の有用性検討)

2 0 1 4

筑波大学大学院博士課程人間総合科学研究科

成田 悠介

**Novel ATP-competitive MEK inhibitor E6201 is effective against vemurafenib-resistant melanoma harboring the MEK1-C121S mutation in a preclinical model**

Yusuke Narita

**Abstract**

Many clinical cases of acquired resistance to the BRAF inhibitor vemurafenib have recently been reported. One of the causes of this acquired resistance is the BRAF downstream kinase point mutation MEK1-C121S. This mutation confers resistance to not only vemurafenib, but also to the allosteric MEK inhibitor selumetinib (AZD6244). Here, we investigated the pharmacological activities and effectiveness of the novel MEK inhibitor E6201 against BRAF-V600E mutant melanoma harboring the MEK1-C121S mutation. A cell-free assay confirmed that E6201 is an ATP-competitive MEK inhibitor meaning it has a different binding mode with MEK compared with allosteric MEK inhibitors. E6201 is more effective against BRAF-V600E mutant

melanoma compared with BRAF wild-type melanoma based on MEK inhibition. We found that the acquired MEK1-C121S mutation in BRAF-V600E mutant melanoma conferred resistance to both vemurafenib and selumetinib but not E6201. The activity of E6201 in this preclinical study is a result of its binding with MEK1 far from the C121S point mutation so the mutation is unable to influence the MAPK pathway inhibitory activity. In conclusion, our preclinical data indicate that E6201 retains its full activity in MEK1-C121S mutated cells.

## **Introduction**

In certain types of cancer, the activation of kinases is known to have a role in oncogenicity (1). Therefore, kinase inhibitors are an attractive option for use as cancer chemotherapy (2). These drugs confer a survival benefit to cancer patients; however, a number of mechanisms of acquired resistance to kinase inhibitors have been reported (3, 4). For example, gatekeeper mutations that confer resistance to kinase inhibitors frequently occur in *EGFR* (5, 6) and *BCR-ABL* (7).

Metastatic melanoma patients have a very poor prognosis with a median survival time of only 6 to 10 months (8). The average annual melanoma rate among Caucasians is about 22 cases per 100,000 people. In comparison, African Americans have an incidence of one case per 100,000 people. Malignant melanoma is the ninth most common cancer in Europe, with more than 100,000 new cases diagnosed in 2012 (3% of the total) and is the 19th most common cancer worldwide, with around 232,000 new cases diagnosed in 2012 (2% of the total). Only Dacarbazine and interleukin-2 (IL-2) were approved as the drugs for metastatic melanoma. Their survival benefit was not substantial (9). Dacarbazine monotherapy produces an overall response rate of 15 to 25%, with an average response time of 5-6 months and complete response rates of 5%. The overall response rate of IL-2 was 16%, including 17 complete responses (CR) (6%)

and 26 partial responses (PR) (10%) (10).

In melanoma, BRAF, PTEN, NRAS, c-kit and MEK mutation is frequently occurred (11). The BRAF-V600E mutation occurs in approximately 50% of melanomas, and this mutation is strongly associated with tumorigenicity (8, 12). The mutation is heterozygous or homozygous and its position is hotspot. The 94-kDa BRAF protein encoded by the gene on chromosome 7q34 functions as a serine/threonine kinase immediately downstream of RAS. BRAF mutations can activate the mitogen-activated protein kinase pathway, leading to uncontrolled proliferation and survival. 80% of all BRAF mutation is occurred. Recently, a clinical trial showed that the BRAF inhibitor vemurafenib conferred significant survival benefit in patients with melanomas harboring BRAF-V600E, and vemurafenib has since been approved by both the United States Food and Drug Administration and the European Medicines Agency (13). However, most patients with melanomas harboring BRAF-V600E progress within 2 to 18 months of the initial response to vemurafenib (14). Unlike with the other kinase inhibitors, no acquired BRAF gatekeeper mutation caused by vemurafenib treatment has been reported in a clinical case; however, there are reports of resistance to vemurafenib mediated through the reactivation of the mitogen-activated protein kinase (MAPK) signaling pathway and the activation of the AKT signaling pathway (15-25).

The MEK1-C121S mutation downstream of *BRAF* is an acquired mutation that has recently been found to confer resistance to vemurafenib (15). This mutation also confers resistance to the allosteric mitogen-activated protein kinase kinase (MEK) inhibitor selumetinib (AZD6244) (15). MEK1-C121S suppresses the MAPK pathway inhibitory activity of vemurafenib and selumetinib (15). Therefore, to improve the clinical outcome of BRAF-V600E melanomas harboring MEK1-C121S, drugs that further inhibit the MAPK pathway are required.

E6201 is a novel MEK inhibitor that we developed (26), and a Phase I clinical trial of E6201 is ongoing in advanced solid tumors (Trial registration ID: NCT00794781). The chemical structure of E6201, a derivative of the natural product f152A1, is markedly different from the representative allosteric MEK inhibitors (Fig. 1). A docking simulation showed that f152A1 binds at the ATP binding site of MEK1 (27); therefore, E6201 is also likely to be an ATP-competitive MEK inhibitor with different pharmacological activities than those of allosteric MEK inhibitors. Furthermore, E6201 merits further investigation for the treatment of BRAF-V600E melanomas harboring MEK1-C121S because of its different MEK binding mode compared with allosteric MEK inhibitors.

Here, we investigated the use of E6201 as a MEK inhibitor against BRAF-V600E

melanoma harboring MEK1-C121S. We show that E6201 is an ATP-competitive MEK inhibitor that has potent growth inhibitory activity in BRAF-V600E melanoma compared with BRAF wild-type (WT) melanoma, although the compound inhibited the MAPK pathway both in BRAF-WT and BRAF-V600E melanoma. Furthermore, we demonstrate that E6201 is active in a preclinical model against BRAF-V600E melanoma harboring MEK1-C121S

## Materials and Methods

### Compounds

Selumetinib and vemurafenib were provided by Wuxi AppTec (Shanghai, China).

### Construction of pENTR\_L1-MEK1-R5 ENTRY vector

pF1KE0668, a plasmid harboring the coding regions of the full-length *MEK1* gene, was purchased from Kazusa DNA Research Institute. The *MEK1* coding region was amplified using the following primer set: attB1\_MEK1-Fwd.,

5'-ggggacaagtttgatacaaaaagcaggctgccaccatgccaagaagaagccgacgccatcc-3';

attB5r\_MEK1-Rev.,

5'-ggggacaactttgtatacaaaagttgtagacgccagcagcatgggttggtgtgctgggc-3'. PCR reactions were performed in a total volume of 50  $\mu$ L containing 10  $\mu$ M of each primer, 0.5 ng of pF1KE0668 as the template DNA, and 1.25 U PrimeSTAR<sup>®</sup> GXL DNA Polymerase (TaKaRa Bio) according to the manufacturer's instructions. PCR reactions were incubated at 98°C for 1 min, followed by 30 cycles of 98°C for 10 s, 60°C for 15 s, and 68°C for 2 min, with a final extension period at 68°C for 5 min. The PCR products (1.3 kbp) were purified from agarose gels using a QIAEX II Gel Extraction Kit (QIAGEN). BP reactions were performed in a total volume of 10  $\mu$ L containing 2  $\mu$ L of BP

Clonase™ II Enzyme Mix, 150 ng pDONR P1-P5r (Invitrogen), and 100 ng PCR product. The reaction was incubated for 2 h at 25°C. After proteinase treatment, the mixture was transformed into *Escherichia coli* TOP10 cells (Invitrogen). Colonies that grew on Lysogeny Broth (LB) plate (containing 50 µg/mL kanamycin) were picked and the insert was sequenced.

### **Site-directed mutagenesis**

pENTR\_L1-MEK1(C121S)-R5, a MEK1-C121S mutant ENTRY vector, was generated by site-directed mutagenesis with a PrimeSTAR® Mutagenesis Basal Kit (TaKaRa Bio) according to the manufacturer's instructions. The primers used were MEK1(C121S)-Fwd., 5'-catgagtccaactctccgtacatcgtgggc-3' and MEK1(C121S)-Rev., 5'-agagttggactcatgcagaacctgcagctc-3'. PCR reactions were performed in a total volume of 50 µL containing 10 µM of each primer, 10 pg of pENTR\_L1-MEK1-R5 as the template DNA, and 25 µL of 2× PrimeSTAR Max Premix. PCR reactions were incubated at 98°C for 1 min, followed by 30 cycles of 98°C for 10 s, 55°C for 15 s, and 72°C for 50 s, with a final extension period at 72°C for 2 min. The PCR product (2.5 µL) was transformed into *E. coli* TOP10 cells (Invitrogen) by using the heat shock method, and recombinants were selected on LB agar media supplemented with 50

μg/mL kanamycin. Two *att*-site sequences and the *MEK1* region were checked by sequencing.

**Construction of pCLxIP\_MEK1 (WT or C121S)-IRES-hmAG vectors (MEK1-internal ribosomal entry site-dependent Azami-Green protein expression vectors)**

pCLxIP\_MEK1-IRES-hmAG vector was constructed by using a MultiSite Gateway® Pro Kit (Invitrogen) according to manufacturer's instructions. pCLxIP-DEST (Cytomegalovirus promoter-based expression vector) and pENTR\_L5-IRES-hmAG-L2 (IRES [internal ribosomal entry site]-dependent Azami-Green protein expression vector) were used in this study. These two vectors were created in-house. MultiSite LR reactions were performed in a 10-μL total volume containing 10 fmoles pENTR\_L1-MEK1-R5, 10 fmoles pENTR\_L5-IRES-hmAG-L2, 20 fmoles pCLxIP-DEST, and 2 μL LR II Clonase™ Plus (Invitrogen). The reaction was incubated overnight at 25°C. After proteinase treatment, the mixture was transformed into *E. coli* TOP10 cells (Invitrogen) by using the heat shock method, and recombinants were selected on LB agar media supplemented with 100 μg/mL ampicillin. The *MEK1* and IRES-hmAG regions were checked by sequencing. A MEK1-C121S mutant

expression vector (pCLxIP\_MEK1[C121S]-IRES-hmAG) was constructed via the same method. These expression vectors were designed so that the IRES-dependent Azami-Green gene and puromycin resistance gene were co-expressed with the *MEK1* gene.

### **Cell lines and cell cultures**

The human melanoma cell lines HMV-1 and SEKI were obtained from the Japanese Collection of Research Bioresources in 1987. The human melanoma cell lines HMCB, CHL-1, MDA-MB435S, and A375 were obtained from the American Type Culture Collection in 2008, 2008, 1998 and 2010 respectively. The melanoma cell line G-361 was obtained from DS Pharma Biomedical in 2010. A375/MEK1 WT and A375/MEK1-C121S cells were prepared by stable transfection of MEK1 WT- or C121S-expressing plasmids into parental A375 cells. HMV-1, SEKI, MDA-MB435S, and A375 cell lines were cultured in RPMI-1640 containing 10% FBS. HMCB and CHL-1 cell lines were cultured in Dulbecco's modified Eagle's medium containing 10% FBS. G-361 cell line was cultured in McCoy's medium containing 10% FBS. All cell lines were cultured at 37°C under a humidified atmosphere containing 5% CO<sub>2</sub>, and authenticated by short-tandem repeat analysis.

## **BRAF DNA Sequencing**

BRAF mutation status was assessed by using next-generation sequencing technology.

Reverse transcribed cDNAs were prepared from HMV-1, HMCB, CHL-1, A375, SEKI,

MDA-MB435S, and G361 cell lines and then used as templates for amplification of

several genes of interest, including *BRAF*. Because it was difficult to amplify full-length

BRAF cDNA, three pairs of primers that together cover the whole BRAF cDNA coding

region were used (sense primer 1: GCCCCGGCTCTCGGTTATAAGATG, antisense

primer 1: CCGTTCCCCAGAGATTCCAA; sense primer 2:

TGCCATTCCGGAGGAGGTGT, antisense primer 2:

GCCCATCAGGAATCTCCCAA; sense primer 3: ATCTGGATCATCCCCTTCCGC,

antisense primer 3: CCCGGAACAGAAAGTAAAGCCTCTAG). PCR products from

each cell line were mixed, and a library was constructed by using a Genomic DNA

Sample Prep Kit (Illumina). Sequencing data were produced by using a Genome

Analyzer II (Illumina) and Standard Cluster Generation and 36 Cycle Sequencing kits

(Illumina).

## **Western blot analysis**

Cells were incubated with a serial dilution of the test compounds in complete medium at 37°C for 24 h. Cells were lysed with cell lysis buffer (Cell Signaling Technology) containing 1 mM phenylmethylsulfonyl fluoride. Cellular debris was removed by centrifugation at 15,000 g for 20 min at 4°C. Western blotting was performed as described (28). Supernatants containing 10 µg of protein were subjected to SDS-PAGE under reducing conditions. The proteins were then transferred onto polyvinylidene fluoride membranes (Millipore) blocked with TBS containing 0.05% Tween-20 and 5% skim milk. The membranes were then probed with the following antibodies: anti-phospho Erk1/2 (Thr202/Tyr204), anti-ERK1/2 (Cell Signaling Technology), and anti-Cyclin D1 (BD Biosciences). Immunoreactive bands were visualized by detecting chemiluminescence with a ChemiDoc XRS gel imaging system (BIO-RAD).

### **Cell proliferation assay**

Cells ( $2 \times 10^3$  cells/100 µL/well) were seeded in 96-well culture plates. After overnight incubation at 37°C under a humidified atmosphere containing 5% CO<sub>2</sub>, various concentrations of each compound were added, and cultured for 3 days. Then, 10 µL of WST-8 reagent (Dojindot) was added to each well, and absorbance was measured at 450 nm by using an Envision multilabel plate reader (Perkinelmer) and compared

with a reference measurement at 665 nm.

### ***In vitro* MEK1 and MEK2 kinase assay**

An ELISA assay kit containing MEK1 and MEK2 recombinant protein was purchased from Carna Biosciences. The assay was performed according to Carna Biosciences' internal protocol.

### **Immunocytochemistry**

A375 cells were seeded ( $5 \times 10^5$  cells/100  $\mu$ L/well) in six-well plates the day before transfection. The cells were transfected with *MEK1* expression vectors using lipofectamine 2000 (Invitrogen) according to the manufacturer's protocol. The following day, the cells were harvested by trypsinization and seeded ( $2.5 \times 10^4$  cells/well) in 96-well imaging plates (BD falcon). After overnight incubation at 37°C under a humidified atmosphere containing 5% CO<sub>2</sub>, the cells were treated with serial dilutions of the test compounds for 24 h. For immunostaining, the cells were fixed with 2% paraformaldehyde for 45 min and permeabilized with 100% MeOH for 10 min. After blocking with 1% bovine serum albumin (BSA)/PBS for 3 h, the cells were incubated overnight with rabbit anti-Cyclin D1 (Abcam) in 0.1% BSA/PBS at 4°C.

After being washed with PBS, the cells were incubated with Alexa568-conjugated anti-rabbit IgG (Invitrogen) and 10  $\mu\text{g/ml}$  Hoechst 33342 (Invitrogen) in 0.1% BSA/PBS for 1 h and then washed with PBS.

Image acquisition for each well was performed on an IN Cell Analyzer 1000 (GE Healthcare) by using a  $\times 20$  objective lens with 360-, 475-, and 555-nm excitation filters monitored through 460-, 517-, and 620-nm emission filters, respectively. The Cyclin D1 expression level of the vector-transfected Azami-Green-positive cells was determined by using the IN Cell Developer software (GE Healthcare). Images collected from 460-nm emission filters were used to define nuclear regions. The Azami-Green expression level and Cyclin D1 expression level of each cell were defined as the level of 517-nm and 620-nm intensity in the nuclear region, respectively. The mean and SD background value at 517-nm intensity was determined by analyzing wells that did not contain cells. Cells with Azami-Green expression levels higher than mean +  $8 \times \text{SD}$  of the background value at 517-nm intensity were defined as Azami-Green-positive. The Cyclin D1 expression level of each well was determined as the median Cyclin D1 expression level of Azami-Green-positive cells in the well.

### **Protein structure and docking simulations with MEK1 protein**

## 1) Homology modeling of protein structure

The coordinates for human-MEK1 and the allosteric inhibitor G-894 complex were obtained from the Research Collaboratory for Structural Bioinformatics Protein Data Bank (PDB entry code: 3V04) (29), and the protein structure was prepared by using the Maestro software package (Schrödinger). Hydrogen atoms were added and a brief relaxation was performed on each starting structure using the Protein Preparation module in the Maestro software. These coordinates were used for the selumetinib docking simulation. For the E6201 simulation, a MEK1 model was built by using the Prime homology modeling program (30, 31) and the human-ERK2 crystal structure (PDB entry code: 2E14) (32) coordinates as the template structure.

## 2) Induced-fit docking simulation

The Induced-Fit Docking (IFD) (33) module in the Maestro software was used. IFD uses the Glide docking program (34) to account for ligand flexibility, as well as the refinement module. The Prime algorithm is implemented in Glide to account for the flexibility of the receptor. Residues within 10 Å of the ligand poses were minimized to form suitable pose conformations at the binding site. Finally, each ligand was redocked to its corresponding low-energy protein structures and the resulting complexes were ranked according to their GlideScore. The IFD, given in kilocalories per mole, was

computed based on the GlideScore and a small fraction of the Prime energy by using the following formula: IFD Score = GlideScore + 0.05 Prime energy.

## **Results**

### **E6201 is an ATP-competitive MEK1 and MEK2 inhibitor**

To determine whether E6201 is an ATP-competitive or -noncompetitive MEK inhibitor, the inhibitory activity of E6201 on MEK1 and MEK2 was evaluated by using a cell-free kinase assay with various concentrations of ATP (Fig. 2). The IC<sub>50</sub> values of E6201 in the MEK1 cell-free assay were 0.020, 0.12, and 1.4 μM at ATP concentrations of 10, 30, and 100 μM, respectively. The IC<sub>50</sub> values in the MEK2 cell-free assay were 0.028, 0.067, and 0.70 μM at ATP concentrations of 10, 30, and 100 μM, respectively. The inhibitory activity of E6201 decreased with increasing ATP dose indicating that E6201 is an ATP-competitive MEK1 and MEK2 inhibitor.

### **Efficacy of E6201 against BRAF-V600E or -WT melanoma**

BRAF-V600E melanoma is reported to be more sensitive than BRAF-WT melanoma to the MAPK pathway inhibition caused by BRAF inhibitors or allosteric MEK inhibitors (35, 36). To assess whether E6201 shows selective growth suppression in BRAF-V600E melanoma, we prepared a melanoma cell-line panel comprising three BRAF-WT (CHL-1, HMCB, and HMV-1) and four BRAF-V600E melanoma cell lines

(G361, MDA-MB435, SEKI and A375). The *BRAF* mutation status of these cell lines was confirmed by DNA sequencing. Cell lines harboring the BRAF-V600E mutation were more sensitive to vemurafenib and selumetinib compared with BRAF-WT cell lines (Fig. 3A). E6201 also showed potent growth inhibitory activity in BRAF-V600E melanoma cell lines compared with BRAF-WT cell lines.

Next, we examined the MAPK pathway inhibitory activity of E6201 in a BRAF-V600E mutant (A375 and G361) and BRAF-WT melanoma (HMV-1) cell line (Fig. 3B and Supplementary Fig. S1). Vemurafenib inhibited extracellular signal-regulated kinase (ERK) phosphorylation in the BRAF-V600E mutant but not in the BRAF-WT melanoma (Fig. 3B), whereas selumetinib inhibited ERK phosphorylation in both the BRAF-V600E mutant and the BRAF-WT melanoma. E6201 also inhibited ERK phosphorylation in both the BRAF-V600E mutant and the BRAF-WT melanoma (Fig. 3B and Supplementary Fig. S1). E6201 inhibited ERK phosphorylation at a lower dose in the BRAF-V600E mutant than in the BRAF-WT melanoma; whereas selumetinib inhibited ERK phosphorylation in the BRAF-V600E mutant at approximately the same dose as in the BRAF-WT melanoma. These results indicate that the growth inhibitory activity of E6201 in melanoma cell lines harboring the BRAF-V600E mutation is mediated via MEK inhibition.

### **E6201 effectiveness on cells transiently or constitutively expressing MEK1-C121S**

MEK1-C121S point mutation confers resistance to both vemurafenib and selumetinib (12). E6201 is an ATP-competitive MEK inhibitor that binds to MEK1 or MEK2 differently from allosteric MEK inhibitors. E6201 may therefore be active against BRAF-V600E melanomas harboring MEK1-C121S.

To assess whether MEK1-C121S confers resistance to E6201 in melanoma cells, we transiently transfected A375 human melanoma cells with a MEK1-C121S-expressing vector. A375 was used because this cell line is reported to harbor the BRAF-V600E mutation and has frequently been used in similar experiments (15, 37). The presence of the BRAF-V600E mutation in A375 was confirmed by DNA sequencing. After treatment with the test compounds, transfected cells were immunocytochemically stained for Cyclin D1, which is a marker of the cytostatic effect of MAPK inhibitors (35, 38, 39). Only about 10% of cells were transfected with expression vectors in our transfection protocol, so to be able to identify transfected cells, we designed expression vectors for the co-expression of the IRES-dependent Azami-Green and *MEK1* genes. We quantified the expression of Cyclin D1 in Azami-Green-negative and -positive (exogenous MEK1-WT/C121S-negative and -positive) cells separately by using an IN

Cell Analyzer high-content analysis system. Cyclin D1 expression decreased after treatment with 3.3  $\mu$ M vemurafenib or 1.1  $\mu$ M selumetinib in almost all of the Azami-Green-negative cells, but not in all of the Azami-Green-positive cells (Fig. 4A). However, Cyclin D1 expression decreased after treatment with 1.1  $\mu$ M E6201 in both the Azami-Green-positive and -negative cells. Quantitatively, the Cyclin D1 expression inhibitory activities of vemurafenib and selumetinib in Azami-Green-positive cells (exogenous MEK1-C121S-positive cells) were remarkably lower compared with that in Azami-Green-negative cells (exogenous MEK1-C121S-negative cells) (Fig. 4B). The Cyclin D1 expression inhibitory activity of vemurafenib and selumetinib in Azami-Green-positive cells (exogenous MEK1-WT-positive cells) did not change compared with that in Azami-Green-negative cells (exogenous MEK1-WT-positive cells) (Supplementary Fig. S2). In contrast, the Cyclin D1 expression inhibitory activity of E6201 in Azami-Green-positive (exogenous MEK1-WT or C121S-positive) cells barely changed compared with Azami-Green-negative (exogenous MEK1-WT- or C121S-negative) cells (Fig. 4 and Supplementary Fig. S2). Moreover, the same result was obtained by using G361 (Supplementary Fig. S3). In A375 and G361, apoptosis was not induced by MAPK inhibition. (Supplementary Fig. S4)

Next, to confirm the result of the transient transfection experiments regarding growth

inhibition, stable MEK1-WT or -C121S transfectants were established by using the A375 cell line. The growth inhibitory activities of vemurafenib and selumetinib in the MEK1-C121S transfectants were approximately 10 times weaker than in the MEK1-WT transfectants (Fig. 5A). However, that of E6201 in the MEK1-C121S transfectant was that same as that in the MEK1-WT transfectants (Fig. 5A). These results indicate that the MEK1-C121S mutation confers resistance to both vemurafenib and selumetinib but not E6201.

#### **Mechanism of acquired vemurafenib and selumetinib resistance and effectiveness of E6201 against MEK1-C121S melanoma**

To confirm the mechanism of vemurafenib and selumetinib resistance and the effectiveness of E6201 against MEK1-C121S mutant melanoma, ERK phosphorylation inhibitory activity was assessed in A375 MEK1-WT and -C121S transfectants (Fig. 5B). The ERK phosphorylation inhibitory activities of vemurafenib and selumetinib in the MEK1-C121S transfectant were approximately 10 times lower than those in the MEK1-WT transfectants. In contrast, the inhibitory activity of E6201 in the MEK1-C121S transfectants was the same as that in the MEK1-WT transfectants. These results indicate that vemurafenib and selumetinib resistance and the effectiveness of

E6201 against MEK1-C121S mutant melanoma is caused by inhibition of the MAPK pathway.

Both selumetinib and E6201 are MEK inhibitors; however, the MEK1-C121S mutation confers resistance only to selumetinib. To elucidate why this difference occurs, we simulated the docking process between selumetinib or E6201 and MEK1. The most energy-stable models are presented in Figure 6. Selumetinib binds to a hydrophobic pocket adjacent to the ATP binding site, like other allosteric inhibitors. (37) This hydrophobic pocket includes residues from both  $\alpha$ -helix C and the activation loop. The binding of allosteric inhibitors within this pocket prevents the structural reorganization of  $\alpha$ -helix C and other motifs, which generates a catalytically active MEK1 conformation.  $\alpha$ -Helix C contains Cys<sub>121</sub>, so Cys<sub>121</sub> mutations may cause resistance either by direct interference or by alteration of the C helix conformation. E6201, however, binds at the ATP binding site, meaning that Cys<sub>121</sub> mutations are unable to affect its inhibitory activity. These results indicate that the different actions of selumetinib and E6201 in BRAF-V600E melanoma result from the different binding modes to MEK 1.

## **Discussion**

On the basis of its MEK inhibitory activity, E6201 was shown here to be an ATP-competitive MEK inhibitor that is active against BRAF-V600E melanoma in a preclinical setting. Furthermore, we showed that E6201 is active in a preclinical model against BRAF-V600E melanoma harboring the MEK1-C121S mutation. Almost all of the MEK inhibitors previously reported are allosteric inhibitors, not ATP-competitive inhibitors (40). Our docking simulation showed that E6201 and selumetinib bind to different sites when they dock with MEK1. These results suggest that the inhibitory mode of action of E6201 is different from that of allosteric MEK inhibitors.

The MEK1-C121S mutation, which confers resistance to vemurafenib, increases MEK activity independently from BRAF and also confers resistance to the allosteric MEK inhibitor selumetinib (15). Our docking simulation showed that the MEK1-C121S mutation induced by vemurafenib treatment is located where selumetinib binds with MEK1, but is far from where E6201 binds with MEK1. This may account for the selumetinib resistance in BRAF-V600E melanoma harboring the MEK1-C121S mutation. In contrast, E6201 suppressed ERK phosphorylation and inhibited cell growth equivalently in BRAF-V600E melanoma harboring MEK1-C121S and in WT melanoma cells. Thus, this is the first paper showing that E6201 potentially retains

anti-cancer activity against melanomas with acquired resistance to vemurafenib associated with the MEK1-C121S mutation.

A combination therapy clinical trial in melanoma using a BRAF inhibitor together with an allosteric MEK inhibitor is ongoing (Trial registration ID: NCT01072175, NCT01271803); however, this combination may not be effective upon acquisition of the MEK1-C121S mutation because the mutation confers resistance to both BRAF inhibitors and allosteric MEK inhibitors. On the basis of this clinical information, the combination of vemurafenib and E6201 may lead to a prolonged response compared with vemurafenib by inhibiting acquisition of the MEK1-C121S mutation in vitro and in vivo preclinical model.

The clinical benefit of trametinib monotherapy (an allosteric MEK inhibitor) was demonstrated in BRAF mutant melanoma with a V600E or V600K BRAF mutation (38). Trametinib was approved by both the United States Food and Drug Administration and the European Medicines Agency (13) for the treatment of patients with unresectable or metastatic melanoma harboring the BRAF-V600E mutation. In the near future, a MEK mutation induced by trametinib treatment may appear as has occurred with the other kinase inhibitors. Acquired resistance to allosteric MEK inhibitors through MEK1 mutations has been reported in a preclinical study (39). Some of these mutations are at

the allosteric binding site. E6201 may be active against melanomas with these mutations because the binding mode of E6201 to MEK1 is different from that of allosteric MEK inhibitors. Further preclinical investigation may be important to prove this hypothesis.

In addition to MEK1-C121S mutation, BRAF inhibitor resistance mechanisms were reported. These include MEK1 mutation, BRAF amplification, NRAS mutation, PDGFR $\beta$  overexpression, COT overexpression, IGF1R activation, dimerization of aberrantly spliced BRAF V600E, FGFR3 activation, KRAS mutation and up regulation of FOXD3 (15-23). The chemotherapies that overcome each class of acquired resistance are required. Therefore, the resistant mechanisms have to be identified to select corrective therapy.

Recently, MEK1 C121S mutation is discovered in hairy-cell leukemia variant (41) and Langerhans cell histiocytosis (42). E6201 may be active if growth and apoptosis depend on MAPK pathway in this leukemia.

In previous report, MEK inhibitor is active in KRAS and NRAS mutated cells in addition to BRAF mutated cells because MAPK pathway is activated and growth is depend on this pathway in these cells. BRAF, NRAS and KRAS mutation are frequently occurred in colorectal cancer, thyroid cancer, pancreatic cancer, lung cancer and melanoma. Therefore, E6201 may be active in these cells.

We show here that the inhibitory activity of E6201 was higher in BRAF-V600E melanoma than in BRAF-WT melanoma, whereas that of selumetinib in BRAF-V600E was the same as in BRAF-WT. This inhibitory selectivity of E6201 against BRAF-WT and BRAF-V600E may lead to a broader therapeutic window because of its weak activity in BRAF-WT cells. Further investigation about activity and toxicity is needed in vivo preclinical study.

In conclusion, this preclinical study demonstrates that E6201, an ATP-competitive MEK inhibitor, retains full activity in BRAF inhibitor or allosteric MEK inhibitor resistant cancer cells.

## References

1. Tsatsanis C, Spandidos DA. Oncogenic kinase signaling in human neoplasms. *Ann N Y Acad Sci.* 2004;1028:168-75.
2. Grant SK. Therapeutic protein kinase inhibitors. *Cell Mol Life Sci.* 2009;66:1163-77.
3. Yauch RL, Settleman J. Recent advances in pathway-targeted cancer drug therapies emerging from cancer genome analysis. *Curr Opin Genet Dev.* 2012;22:45-9.
4. Barouch-Bentov R, Sauer K. Mechanisms of drug resistance in kinases. *Expert Opin Investig Drugs.* 2011;20:153-208.
5. Engelman JA, Settleman J. Acquired resistance to tyrosine kinase inhibitors during cancer therapy. *Curr Opin Genet Dev.* 2008;18:73-9.
6. Hammerman PS, Janne PA, Johnson BE. Resistance to Epidermal Growth Factor Receptor Tyrosine Kinase Inhibitors in Non-Small Cell Lung Cancer. *Clin Cancer Res.* 2009;15:7502-9.
7. Milojkovic D, Apperley J. Mechanisms of Resistance to Imatinib and Second-Generation Tyrosine Inhibitors in Chronic Myeloid Leukemia. *Clin Cancer Res.* 2009;15:7519-27.

8. Chapman PB, Hauschild A, Robert C, Haanen JB, Ascierto P, Larkin J, et al. Improved survival with vemurafenib in melanoma with BRAF V600E mutation. *N Engl J Med*. 2011;364:2507-16.
9. Flaherty KT, Yasothan U, Kirkpatrick P. Vemurafenib. *Nat Rev Drug Discov*. 2011;10:811-2.
10. Foletto MC, Haas SE. Cutaneous melanoma: new advances in treatment. *An Bras Dermatol*. 2014;89:301-10.
11. Mehnert JM, Kluger HM. Driver mutations in melanoma: lessons learned from bench-to-bedside studies. *Curr Oncol Rep*. 2012;14:449-57.
12. Hoeflich KP, Gray DC, Eby MT, Tien JY, Wong L, Bower J, et al. Oncogenic BRAF is required for tumor growth and maintenance in melanoma models. *Cancer Res*. 2006;66:999-1006.
13. Ascierto PA, Kirkwood JM, Grob JJ, Simeone E, Grimaldi AM, Maio M, et al. The role of BRAF V600 mutation in melanoma. *J Transl Med*. 2012;10:85.
14. Tuma RS. Getting around PLX4032: studies turn up unusual mechanisms of resistance to melanoma drug. *J Natl Cancer Inst*. 2011;103:170-1, 7.

15. Wagle N, Emery C, Berger MF, Davis MJ, Sawyer A, Pochanard P, et al. Dissecting therapeutic resistance to RAF inhibition in melanoma by tumor genomic profiling. *J Clin Oncol.* 2011;29:3085-96.
16. Shi H, Moriceau G, Kong X, Lee MK, Lee H, Koya RC, et al. Melanoma whole-exome sequencing identifies (V600E)B-RAF amplification-mediated acquired B-RAF inhibitor resistance. *Nat Commun.* 2012;3:724.
17. Nazarian R, Shi H, Wang Q, Kong X, Koya RC, Lee H, et al. Melanomas acquire resistance to B-RAF(V600E) inhibition by RTK or N-RAS upregulation. *Nature.* 2010;468:973-7.
18. Johannessen CM, Boehm JS, Kim SY, Thomas SR, Wardwell L, Johnson LA, et al. COT drives resistance to RAF inhibition through MAP kinase pathway reactivation. *Nature.* 2010;468:968-72.
19. Villanueva J, Vultur A, Lee JT, Somasundaram R, Fukunaga-Kalabis M, Cipolla AK, et al. Acquired resistance to BRAF inhibitors mediated by a RAF kinase switch in melanoma can be overcome by cotargeting MEK and IGF-1R/PI3K. *Cancer Cell.* 2010;18:683-95.
20. Poulikakos PI, Persaud Y, Janakiraman M, Kong X, Ng C, Moriceau

G, et al. RAF inhibitor resistance is mediated by dimerization of aberrantly spliced BRAF(V600E). *Nature*. 2011;480:387-90.

21. Basile KJ, Abel EV, Aplin AE. Adaptive upregulation of FOXD3 and resistance to PLX4032/4720-induced cell death in mutant B-RAF melanoma cells. *Oncogene*. 2012;31:2471-9.

22. Yadav V, Zhang X, Liu J, Estrem S, Li S, Gong XQ, et al. Reactivation of Mitogen-activated Protein Kinase (MAPK) Pathway by FGF Receptor 3 (FGFR3)/Ras Mediates Resistance to Vemurafenib in Human B-RAF V600E Mutant Melanoma. *J Biol Chem*. 2012;287:28087-98.

23. Su F, Bradley WD, Wang Q, Yang H, Xu L, Higgins B, et al. Resistance to selective BRAF inhibition can be mediated by modest upstream pathway activation. *Cancer Res*. 2012;72:969-78.

24. Straussman R, Morikawa T, Shee K, Barzily-Rokni M, Qian ZR, Du J, et al. Tumour micro-environment elicits innate resistance to RAF inhibitors through HGF secretion. *Nature*. 2012;487:500-4.

25. Wilson TR, Fridlyand J, Yan Y, Penuel E, Burton L, Chan E, et al. Widespread potential for growth-factor-driven resistance to anticancer kinase inhibitors. *Nature*. 2012;487:505-9.

26. Goto M, Chow J, Muramoto K, Chiba K, Yamamoto S, Fujita M, et al. E6201 [(3S,4R,5Z,8S,9S,11E)-14-(ethylamino)-8,9,16-trihydroxy-3,4-dimethyl-3,4,9,19-tetrahydro-1H-2-benzoxacyclotetradecine-1,7 (8H)-dione], a novel kinase inhibitor of mitogen-activated protein kinase/extracellular signal-regulated kinase kinase (MEK)-1 and MEK kinase-1: in vitro characterization of its anti-inflammatory and antihyperproliferative activities. *J Pharmacol Exp Ther.* 2009;331:485-95.
27. Ikemori-Kawada M, Inoue A, Goto M, Wang YJ, Kawakami Y. Docking Simulation Study and Kinase Selectivity of f152A1 and Its Analogs. *Journal of Chemical Information and Modeling.* 2012;52:2059-68.
28. Matsui J, Funahashi Y, Uenaka T, Watanabe T, Tsuruoka A, Asada M. Multi-kinase inhibitor E7080 suppresses lymph node and lung metastases of human mammary breast tumor MDA-MB-231 via inhibition of vascular endothelial growth factor-receptor (VEGF-R) 2 and VEGF-R3 kinase. *Clin Cancer Res.* 2008;14:5459-65.
29. Heald RA, Jackson P, Savy P, Jones M, Gancia E, Burton B, et al. Discovery of novel allosteric mitogen-activated protein kinase kinase (MEK) 1,2 inhibitors possessing bidentate Ser212 interactions. *J Med Chem.*

2012;55:4594-604.

30. Jacobson MP, Friesner RA, Xiang Z, Honig B. On the role of the crystal environment in determining protein side-chain conformations. *J Mol Biol.* 2002;320:597-608.

31. Jacobson MP, Pincus DL, Rapp CS, Day TJ, Honig B, Shaw DE, et al. A hierarchical approach to all-atom protein loop prediction. *Proteins.* 2004;55:351-67.

32. Ohori M, Kinoshita T, Yoshimura S, Warizaya M, Nakajima H, Miyake H. Role of a cysteine residue in the active site of ERK and the MAPKK family. *Biochem Biophys Res Commun.* 2007;353:633-7.

33. Sherman W, Day T, Jacobson MP, Friesner RA, Farid R. Novel procedure for modeling ligand/receptor induced fit effects. *J Med Chem.* 2006;49:534-53.

34. Friesner RA, Banks JL, Murphy RB, Halgren TA, Klicic JJ, Mainz DT, et al. Glide: a new approach for rapid, accurate docking and scoring. 1. Method and assessment of docking accuracy. *J Med Chem.* 2004;47:1739-49.

35. Solit DB, Garraway LA, Pratilas CA, Sawai A, Getz G, Basso A, et al. BRAF mutation predicts sensitivity to MEK inhibition. *Nature.*

2006;439:358-62.

36. Tsai J, Lee JT, Wang W, Zhang J, Cho H, Mamo S, et al. Discovery of a selective inhibitor of oncogenic B-Raf kinase with potent antimelanoma activity. *Proc Natl Acad Sci U S A*. 2008;105:3041-6.

37. Emery CM, Vijayendran KG, Zipser MC, Sawyer AM, Niu L, Kim JJ, et al. MEK1 mutations confer resistance to MEK and B-RAF inhibition. *Proc Natl Acad Sci U S A*. 2009;106:20411-6.

38. Greger JG, Eastman SD, Zhang V, Bleam MR, Hughes AM, Smitheman KN, et al. Combinations of BRAF, MEK, and PI3K/mTOR inhibitors overcome acquired resistance to the BRAF inhibitor GSK2118436 dabrafenib, mediated by NRAS or MEK mutations. *Mol Cancer Ther*. 2012;11:909-20.

39. Paraiso KH, Fedorenko IV, Cantini LP, Munko AC, Hall M, Sondak VK, et al. Recovery of phospho-ERK activity allows melanoma cells to escape from BRAF inhibitor therapy. *Br J Cancer*. 2010;102:1724-30.

40. Trujillo JI. MEK inhibitors: a patent review 2008 - 2010. *Expert Opin Ther Pat*. 2011;21:1045-69.

41. Waterfall JJ, Arons E, Walker RL, Pineda M, Roth L, Killian JK, et

al. High prevalence of MAP2K1 mutations in variant and IGHV4-34-expressing hairy-cell leukemias. *Nat Genet.* 2014;46:8-10.

42. Brown NA, Furtado LV, Betz BL, Kiel MJ, Weigelin HC, Lim MS, et al. High prevalence of somatic MAP2K1 mutations in BRAF V600E-negative Langerhans cell histiocytosis. *Blood.* 2014;124:1655-8.

#### Figure legends

Figure 1. (A) Structure of E6201. (B) Structure of four allosteric MEK inhibitors.

Figure 2. (A) MEK1 and (B) MEK2 inhibitory activity of E6201 at different concentrations of ATP.

Figure 3. Effect of vemurafenib (BRAF inhibitor), selumetinib (allosteric MEK inhibitor), and E6201 (ATP-competitive MEK inhibitor) on BRAF-WT and -V600E melanoma cell lines. *BRAF* mutation status was confirmed by using DNA sequencing.

(A) Growth inhibitory activity of each compound. White columns represent the result in BRAF-WT cell lines and black columns represent the result in BRAF-V600E cell lines.

The growth IC<sub>50</sub> values of each compound in BRAF-WT melanoma cell lines were all

above 1  $\mu\text{M}$ . (B) MAPK pathway inhibitory activity of the test compounds.

Figure 4. Effect of vemurafenib, selumetinib, or E6201 on Cyclin D1 expression in exogenous MEK1-C121S-positive or -negative A375 cells. (A) Cells were treated with 3.3  $\mu\text{M}$  vemurafenib, 1.1  $\mu\text{M}$  selumetinib, or 1.1  $\mu\text{M}$  E6201. Hoechst is a total cell stain. Azami-Green-positive cells represent exogenous MEK1-C121S-expressing cells. Scale bar represents 100  $\mu\text{m}$ . (B) Quantification of Cyclin D1 expression in exogenous MEK1-C121S-positive or -negative cells after treatment with the test compounds.

Figure 5. Effect of vemurafenib, selumetinib, or E6201 in MEK1-WT or -C121S transfectants. (A) Growth inhibitory activity of the test compounds. (B) MAPK pathway inhibitory activity of each compound.

Figure 6. (A) Most energy-stable complex models. Selumetinib binds to a hydrophobic pocket adjacent to the ATP binding site. (B) Most energy-stable complex model. E6201 binds at the ATP binding site.

Supplementary Figure 1. Effect of vemurafenib, selumetinib, or E6201 on Cyclin D1

expression in exogenous MEK1-WT-positive or -negative A375 cells (A) Cells were treated with 3.3  $\mu$ M vemurafenib, 1.1  $\mu$ M selumetinib, or 1.1  $\mu$ M E6201. Hoechst is a total cell stain. Azami-Green-positive cells represent exogenous MEK1-WT-expressing cells. Scale bar represents 100  $\mu$ m. (B) Quantification of Cyclin D1 expression in exogenous MEK1-WT-positive or -negative cells after treatment with the test compounds.

Supplementary Figure 2. MAPK pathway inhibitory activity of the test compounds in G361.

Supplementary Figure 3. Effect of vemurafenib, selumetinib, or E6201 on Cyclin D1 expression in (A) exogenous MEK1-C121S-positive or -negative G361 cells and in (B) exogenous MEK1-WT-positive or -negative G361 cells.

Supplementary Figure 4. Cleaved -PARP induction in A375 and G361 parental cells.

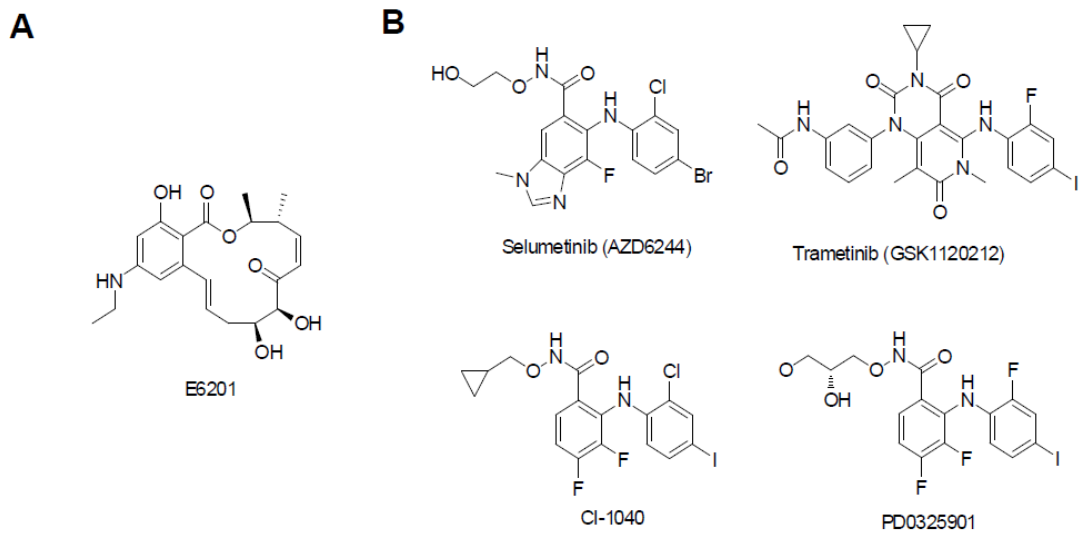


Fig. 1.

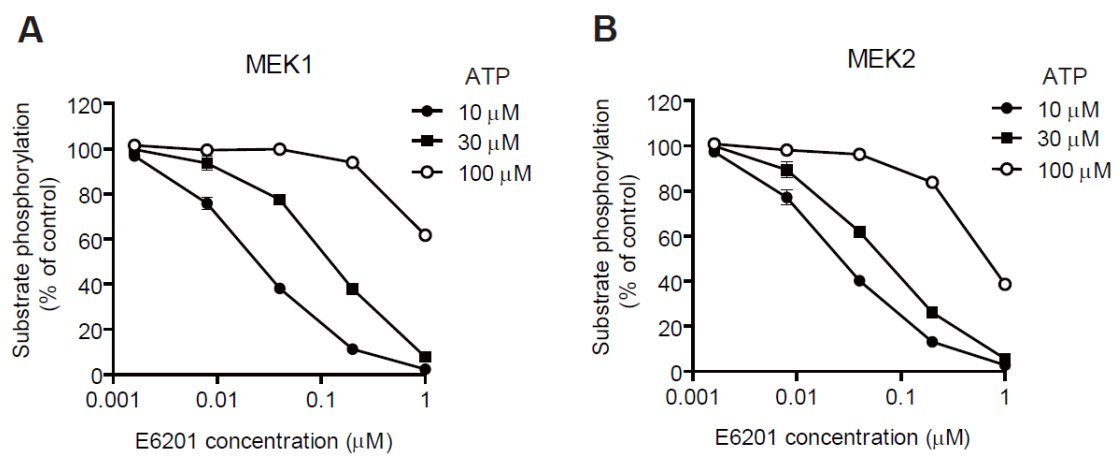


Fig. 2.

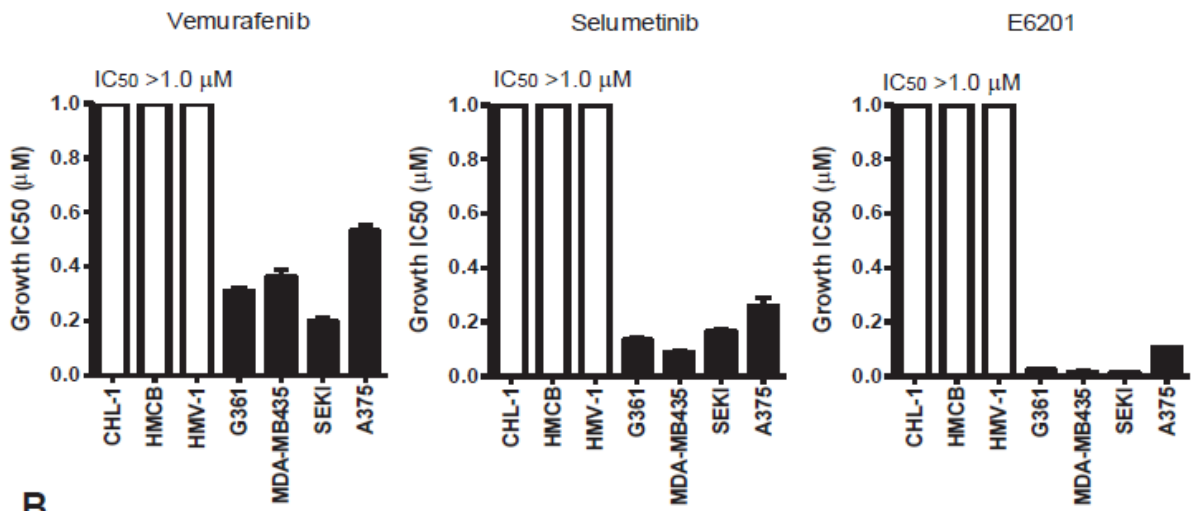
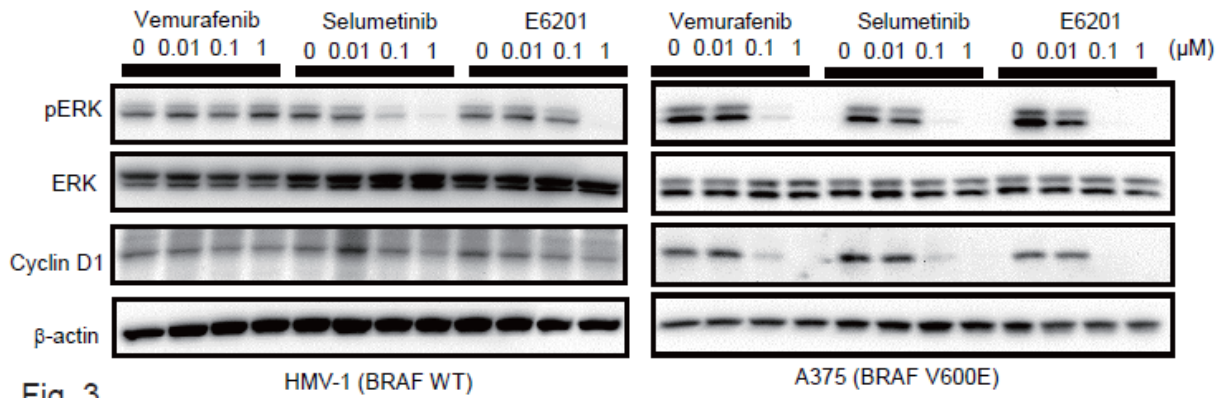
**A****B**

Fig. 3.

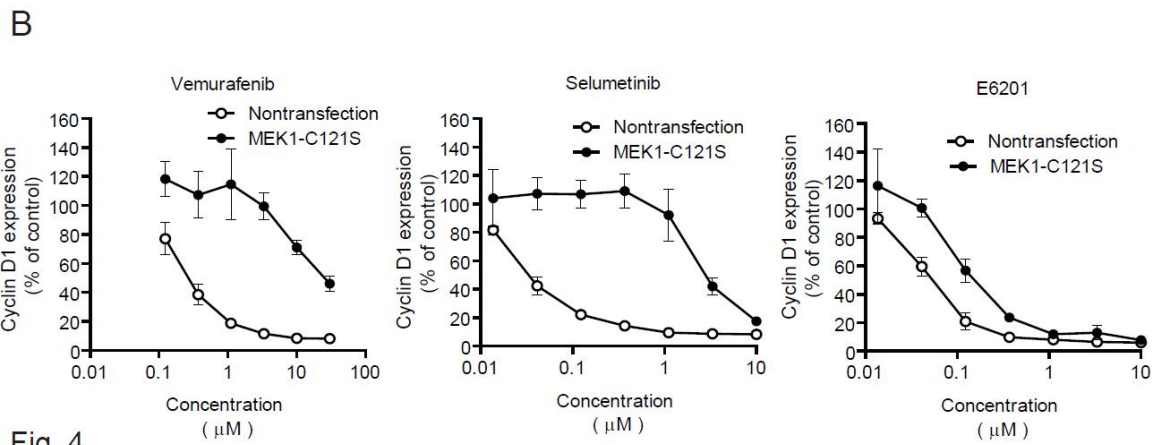
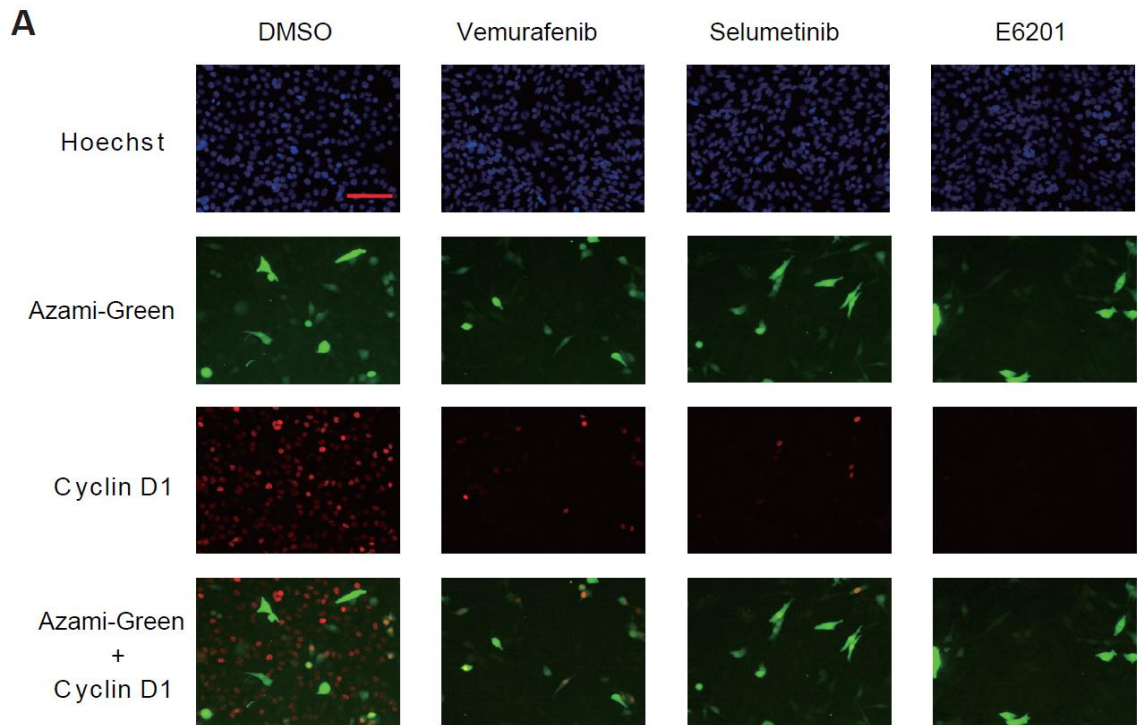


Fig. 4.

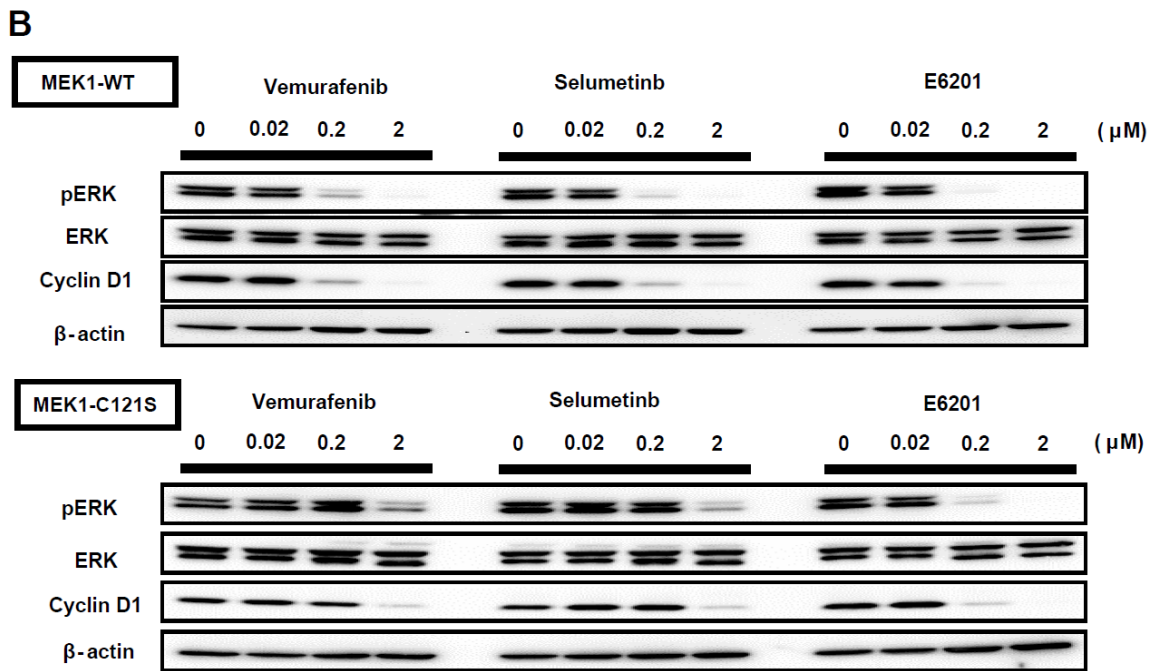
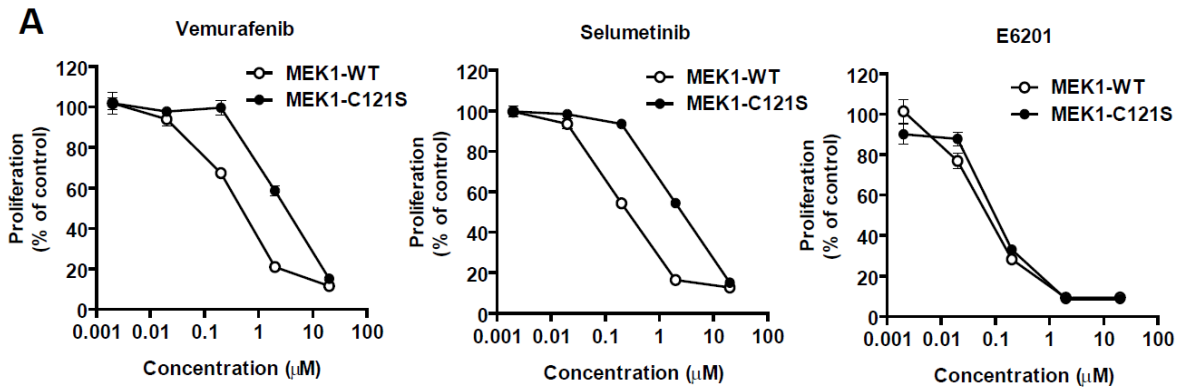


Fig. 5.

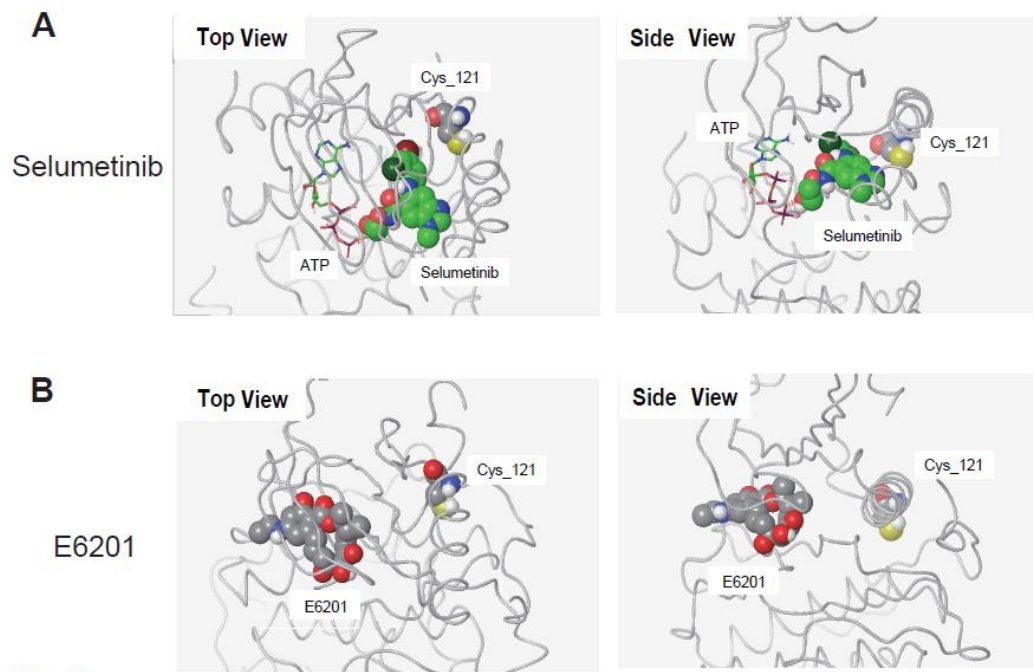


Fig. 6.

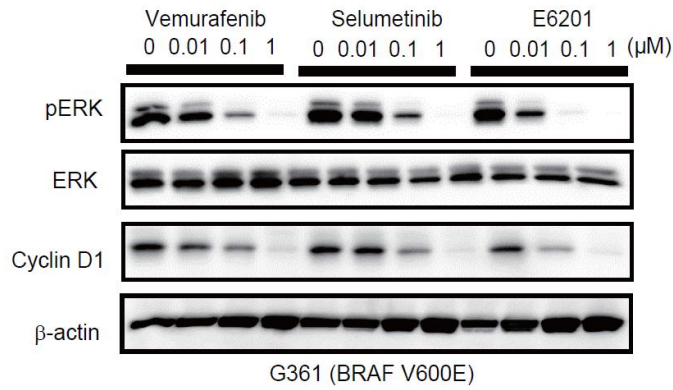


Fig. S1.

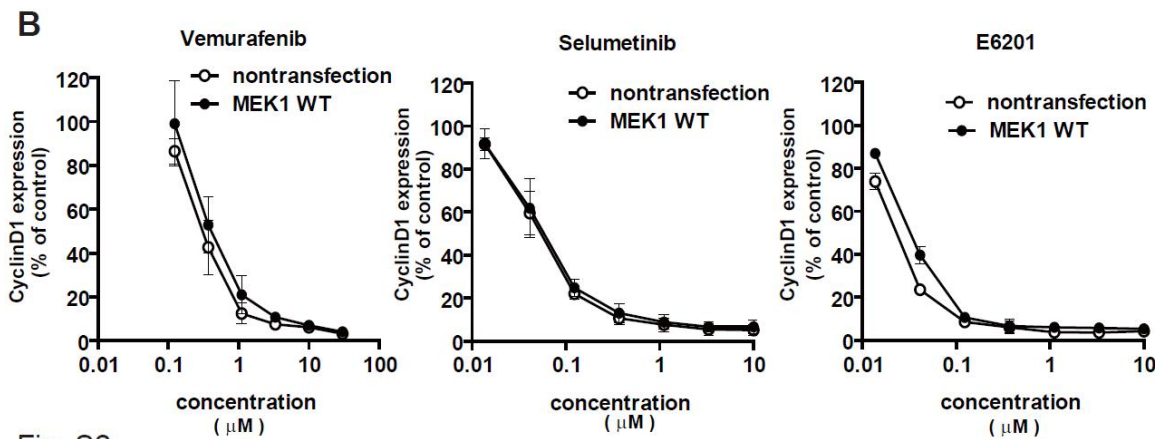
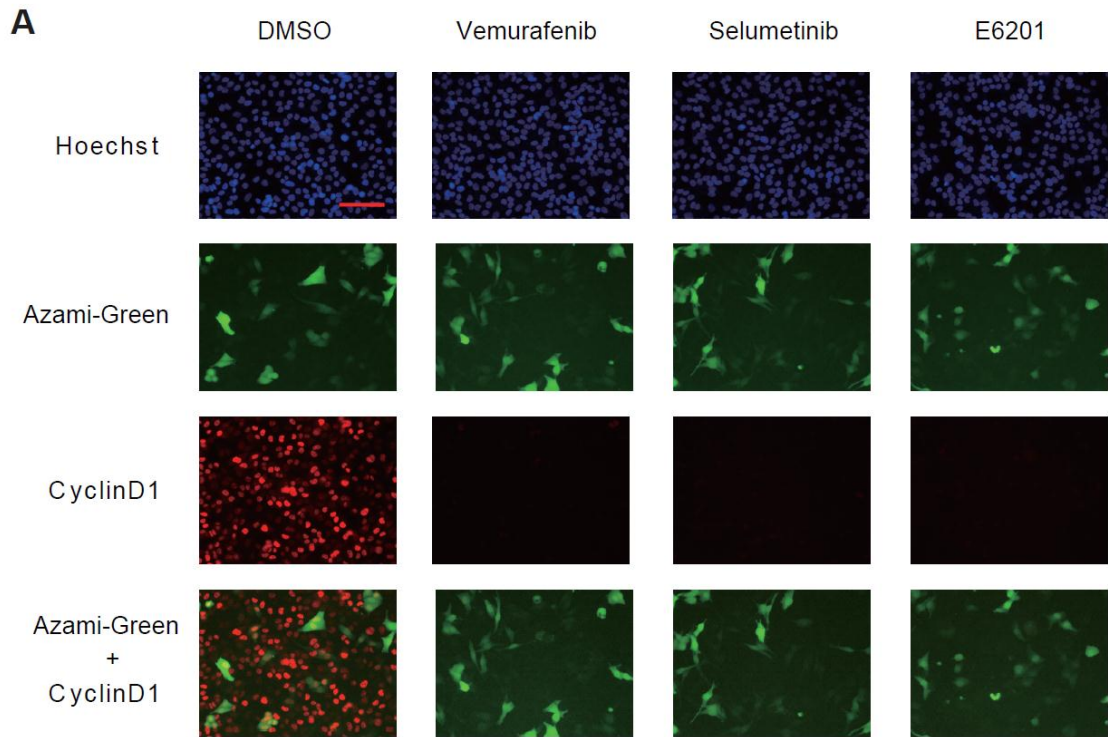


Fig. S2.

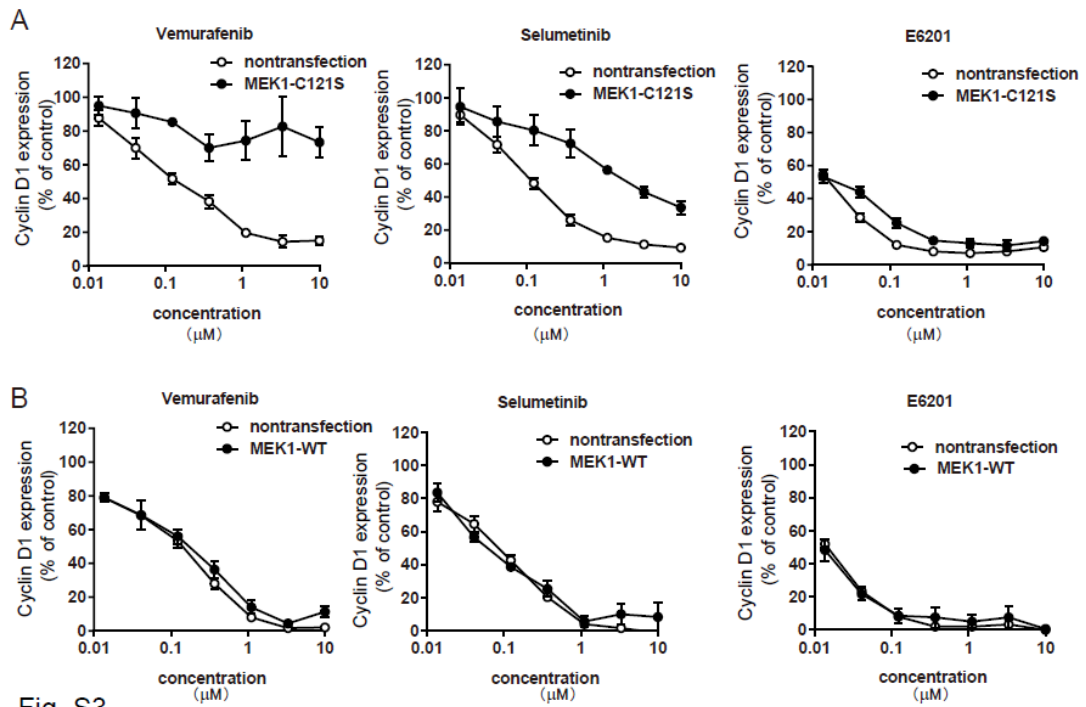


Fig. S3.

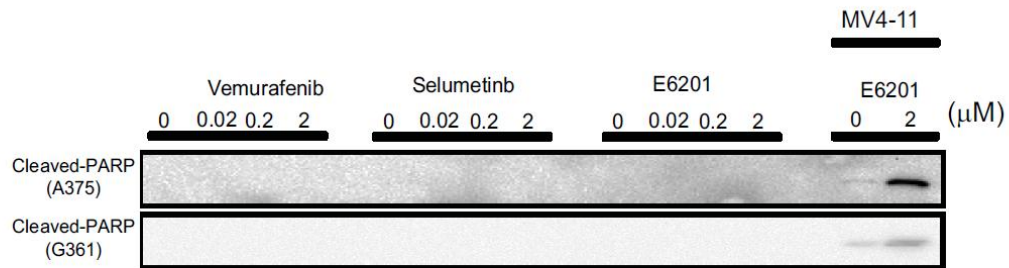


Fig. S4.